Analysis of Cloud-Radiation Interactions Using ARM Observations and a Single-Column Model

S. F. Iacobellis, R. C. J. Somerville, D. E. Lane, and J. Berque
Scripps Institution of Oceanography
University of California
San Diego, California

Introduction

In this study, observations from the Atmospheric Radiation Measurement (ARM) Southern Great Plains' (SGP) site are used to test the realism of results produced by various cloud parameterizations within a single-column model (SCM). The cloud parameterizations differ with regard to the inclusion of cloud liquid water, the specification of the effective cloud droplet radius, and the parameterization of the cloud optical properties (both solar and terrestrial). The SCM is a diagnostic model resembling a single vertical column of a 3-dimensional general circulation model (GCM). The one-dimensional SCM is forced with horizontal advection terms derived from either observations or numerical weather prediction analyses. In this paper, the horizontal advective terms were derived from observations taken during the Summer 1995 (July 18-August 2) and Spring 1996 (April 16-May 5) intensive observation periods (IOPs) at the ARM SGP Cloud and Radiation Testbed (CART) site.

Cloud Parameterizations

Slingo (1987): In this scheme, the stratiform cloud amount depends upon the large-scale relative humidity, vertical velocity and static stability, while convective cloud amount is parameterized as a function of convective mass flux.

Tiedtke (1993): This scheme introduces two new prognostic equations for cloud liquid water/ice and cloud amount. Terms representing the formation of clouds and cloud water/ice due to convection, boundary layer turbulence and stratiform condensation processes are included in these equations. Cloud water/ice is removed (and clouds are dissipated) through evaporation and conversion of cloud droplets and ice to precipitation.

Model Configurations

NOCW: Cloud amount is determined using the Slingo scheme while cloud optical thicknesses are parameterized using model temperature, humidity and pressure following McFarlane et al. (1992).

CWRF: The parameterization of Tiedtke (1993) is used to calculate the cloud liquid water/ice and cloud amounts. Cloud optical thickness is calculated as a function of the cloud water path and effective cloud droplet radius using the formula of Slingo (1989). The cloud droplet radius is fixed at 10 µm.

CWRI: This experiment is the same as CWRF except that the effective cloud droplet radius is parameterized as a function of the liquid water content for water clouds (Bower et al. 1994) and as a function of cloud temperature (Suzuki et al. 1993) for ice clouds.

In all model experiments, cloud infrared (IR) emissivity (ε) is calculated using the formula of Platt and Harshvardhan (1988) $\varepsilon=1.0 - \exp(-0.75 * \tau)$, where τ is the cloud optical thickness. The SCM also employs the cumulus convection scheme of Zhang and McFarlane (1995) and the longwave and shortwave radiation parameterizations of Morcrette (1990) and Fouquart and Bonnel (1980), respectively. A vertical resolution of 19 layers (10 mb near surface; 100 mb in mid-troposphere) and a timestep of 7.5 minutes is used in all SCM model experiments. The model experiments are summarized in Table 1.

Table 1. SCM configurations.

	NOCW	**CWRF**	**CWRI**
Cloud Scheme	Slingo	Tiedtke	Tiedtke
Cloud Water	None	Explicit	Explicit
Cloud Optical Thickness	Specified	Calculated	Calculated
Effective Droplet Radius	Not Applicable	Fixed (10 µm)	Calculated

Time-Averaged Results

Each of the three configurations of the SCM were run using forcing data from the Lawrence Livermore National Laboratory (LLNL) objective analysis data set (derived from ARM measurements) for both Summer 1995 and Spring 1996 IOPs. In these runs, the model temperature and humidity were relaxed to observed values using a time constant of 24 hours.

The mean downwelling surface shortwave flux (DWSF), outgoing longwave radiation (OLR) and total cloud amount from each model run (NOCW, CWRF, and CWRI) for both IOPs (Summer-95 and Spring-96) are shown in Table 2 together with corresponding observed means. The model results show significant variation between the three configurations; however, based on this limited data, it is difficult to determine which of the model configurations produces the most realistic results. Yet, one consistent feature seen in the model results from both IOPs is that larger values of DWSF and OLR are produced by configuration CWRI compared to CWRF. These differences are attributable to the inclusion of an interactive cloud droplet radius in CWRI.

Table 2. Time-averaged results.

	DWSF (W/m^{-2})	OLR (W/m^{-2})	Cloud Fraction
Summer 1995 IOP			
NOCW	282	263	0.43
CWRF	265	253	0.42
CWRI	283	259	0.42
OBS	267	255	0.49
Spring 1996 IOP			
NOCW	290	258	0.29
CWRF	277	246	0.41
CWRI	289	252	0.40
OBS	255	241	0.49

The mean vertical profile of cloud fraction, cloud IR emissivity and cloud extinction (cloud optical depth normalized by layer depth) from the model runs during the Spring 1996 IOP are shown in Figure 1. All three model configurations produce maximum cloudiness in the upper troposphere at approximately 300 mb. It is apparent from this data that the differences in the DWSF and OLR noted above are due to larger values of high cloud extinction and high cloud emissivity by model configuration CWRF compared to CWRI. Future work is planned to evaluate the vertical cloud properties with ARM observations when these measurements become available from future IOPs.

During our analysis, a systematic deficiency in the model cloud results became apparent when the time series of cloud fraction was compared to satellite observations from GOES-8. During the Spring 1996 IOP, there were several events in which large increases in cloud amount were observed. In most instances the model also produced an increase in cloudiness, however the model clouds usually lagged the observations by several hours. In other instances the model did not produce any clouds at all.

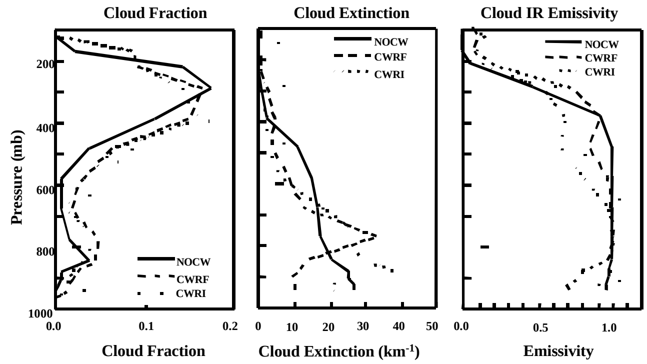

Figure 1. Mean vertical profile of cloud fraction, extinction, and IR emissivity from model runs during the Spring 1996 IOP.

To better understand this model shortcoming, a short 48-hour segment (April 21-22) of the Spring 1996 IOP was further analyzed. The SCM (CWRI configuration) was rerun for the 48-hr period using no correction terms. One reason for choosing this time period was that it was not necessary to use relaxation correction to produce model values of temperature and humidity very close to observed. This indicates that the advection terms provided by the objective analysis schemes are realistic during this time period.

The time-series of several quantities from this 48-hr SCM run are shown in Figure 2 along with corresponding observations. Observations from GOES-8 indicate significant cloudiness on April 20 while the model maintains clear skies. This observed cloudiness is also apparent by concurrent decreases in the observed DWSF and OLR and a concurrent increase in the downwelling surface longwave flux. The relatively modest reduction in the observed downwelling surface shortwave flux and the small values of observed liquid water path indicate that these observed clouds are most likely high optically thin cirrus clouds. Note that cloud base height data from the Belfort laser ceilometer (BLC) (not shown) indicated no clouds on April 20; however, it is quite likely that these clouds were above the 7.5-km range of this instrument.

Analysis of Clouds and Relative Humidity on April 20

One possibility why the SCM does not produce clouds on April 20 is that these clouds were advected into the column overlying the SGP CART site (the advection of cloud water/ice is not included in the forcing terms). A sequence of cloud fraction observations retrieved from the Minnis

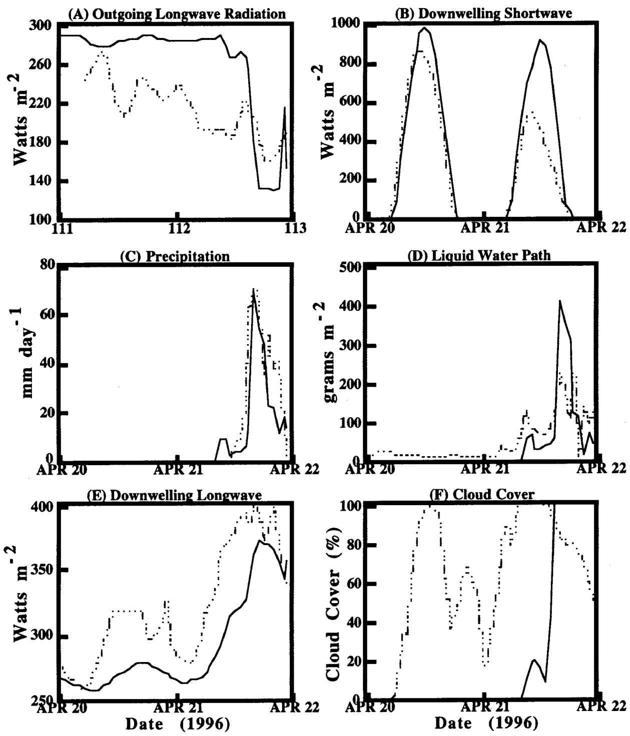

Figure 2. SCM (solid) and observations (dashed).

GOES-8 data products on April 20 covering region 92°W to 104°W and 33°N to 41°N were analyzed. The large increase in cloudiness over the CART site during the morning of April 20 is easily seen in this data; however, it is difficult to determine if the clouds were advected or developed over the CART site. The horizontal moisture advection during this 48-hr period shows a strong moistening of the upper troposphere on the morning of April 20, which would be expected if clouds (i.e., cloud water/ice) were also being advected into the column. Unfortunately, this data is not conclusive evidence that clouds were advected into the area.

Figure 3 shows the vertical profile of relative humidity (RH) at April 20 1130 (local time) at each Balloon Borne Sounding System (BBSS) site and from the SCM. It is interesting to note the significant variability between the RH from the five observation sites. At each of these sites there is a relative maximum of RH located in the upper troposphere during the mid-morning hours of April 20. This relative maximum is also seen in the SCM results. In most relative humidity-based cloud schemes, clouds are not formed until the RH reaches a critical value (usually around 80%). Even in the Tiedtke cloud water scheme the conversion of water vapor into liquid water in stratiform clouds does not start until a critical RH of 80% or greater is achieved. It is surprising to see that in all five of the soundings the RH never is larger than 80% during April 20, even though several independent observations (see Figure 2) suggest the presence of clouds (nearly 100% from GOES-8 measurements). Walcek (1994) has documented the presence of mid-tropospheric clouds (appr. 650 mb) in midlatitude storms when the relative humidity is considerably lower than 80%. Further study is planned to document other short duration events to determine if improvements can be made to the specification of a critical RH perhaps by including other factors (i.e., convective stability and vertical velocity) or by calculating the relative humidity using saturation values with respect to ice.

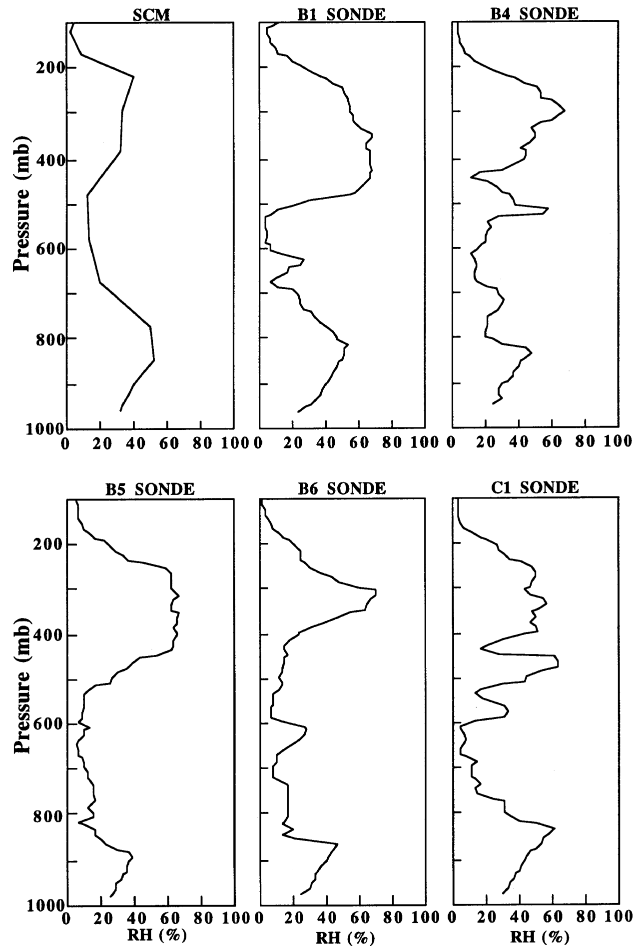

Figure 3. Vertical profile of relative humidity on April 20.

Vertical Resolution

The ARM measurements in Figure 2 indicate that the observed clouds on April 20 are optically thin and may also be geometrically thin. If this is the case, the 19 vertical layers of the SCM may be too coarse to resolve these clouds. To investigate the effects of model vertical resolution, the CWRI configuration of the SCM was rerun during the Spring 1996 IOP with 53 vertical layers (approximate resolution of 25 mb). Figure 4 shows the modeled cloud cover from both the 19 and 53 layer versions of the SCM along with the GOES-8 observations. A significant improvement is seen in the model results when higher vertical resolution is employed. Yet, there are still obvious deficiencies in the model cloud cover, which may be attributable to either the horizontal advection of clouds into the CART site and/or inadequacies of the model physics with regards to the critical relative humidity for the formation of cloud liquid water.

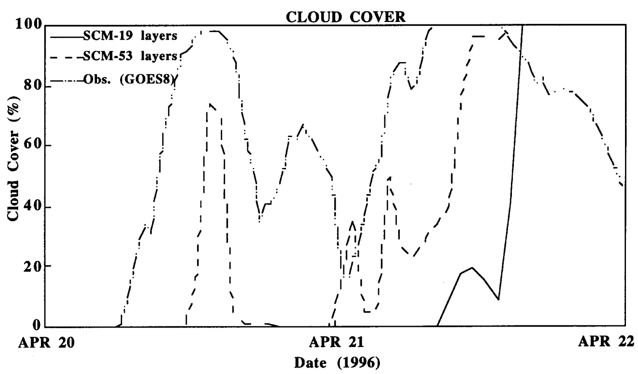

Figure 4. Modeled cloud cover from both the 19 and 53 layer versions of the SCM along with the GOES-8 observations.

Conclusions

- Using an interactive cloud droplet radius decreases the cloud optical thickness and cloud IR emissivity of high clouds, which acts to increase the downwelling surface shortwave flux and the outgoing longwave radiation.

- It is difficult to evaluate the vertical distribution of model-produced cloud extinction, cloud emissivity, cloud liquid water content and effective cloud droplet radius until observations of these quantities are available.

- Future planned measurements of cloud microphysical properties at the ARM SGP site will be an extremely valuable tool to evaluate and improve cloud-radiation parameterizations.

- SCM cloud parameterization often underestimated the observed cloud amount during the Spring 1996 IOP. This underestimation may be due to the horizontal advection of clouds into the model domain.

- Analysis of ARM observations indicates the presence of clouds while the corresponding maximum relative humidity is less than 80%. This implies that the underlying principles of a critical relative humidity of 80% for cloud formation used in most cloud parameterizations may need to be re-examined.

References

Bower, K. N., T. W. Choularton, J. Latham, J. Nelson, M. B. Baker, and J. Jensen, 1994: A parameterization of warm clouds for use in atmospheric general circulation models. *J. Atmos. Sci.*, **51**, 2722-2732.

Fouquart, Y., and B. Bonnel, 1980: Computation of solar heating of the Earth's atmosphere: a new parameterization. *Beitr. Phys. Atmos.*, **53**, 35-62.

McFarlane, N. A., G. J. Boer, J.-P. Blanchet, and M. Lazare, 1992: The Canadian Climate Centre second-generation general circulation model and its equilibrium climate. *J. Climate*, **5**, 1013-1044.

Morcrette, J.-J., 1990: Impact of changes to the radiation transfer parameterizations plus cloud optical properties in the ECMWF model. *Mon. Wea. Rev.*, **118**, 847-873.

Platt, C. M. R., and Harshvardhan, 1988: Temperature dependence of cirrus extinction: Implications for climate feedback. *J. Geophys. Res.*, **93**, 11051-11058.

Slingo, A., 1989: A GCM parameterization for the shortwave radiative properties of water clouds. *J. Atmos. Sci.*, **46**, 1419-1427.

Slingo, J. M., 1987: The development and verification of a cloud prediction scheme for the ECMWF model. *Q. J. R. Meteorol. Soc.*, **113**, 899-927.

Suzuki, T., M. Tanaka, and T. Nakajima, 1993: The microphysical feedback of cirrus cloud in climate change. *J. Meteor. Soc. Japan*, **71**, 701-713.

Tiedtke, M., 1993: Representation of clouds in large-scale models. *Mon. Wea. Rev.*, **121**, 3040-3061.

Walcek, C. J., 1994: Cloud cover and its relationship to relative humidity during a springtime midlatitude cyclone. *Mon. Wea. Rev.*, **122**, 1021-1035.

Zhang, G. J., and N. A. McFarlane, 1995: Sensitivity of climate simulations to the parameterization of cumulus convection in the Canadian Climate Centre general circulation model. *Atmos-Ocean*, **33**, 407-446.

Recent Publications from This Project

Byrne, R. N., R. C. J. Somerville, and B. Subasilar, 1996: Broken-cloud enhancement of solar radiation absorption. *J. Atmos. Sci.*, **53**, 878-886.

Iacobellis, S. F., and R. C. J. Somerville, 1998: Implications of microphysics for cloud-radiation parameterizations: Lessons from TOGA-COARE. Submitted to the *J. Atmos. Sci.*

Lee, W.-H., S. F. Iacobellis, and R. C. J. Somerville, 1997: Cloud radiation forcings and feedbacks: General circulation model tests and observational validation. *J. Climate*, **10**, 2479-2496.

Lee, W.-H., and R. C. J. Somerville, 1996: Effects of alternative cloud radiation parameterizations in a general circulation model. *Ann. Geophyci.*, **14**, 107-114.

Randall, D. A., K.-M. Xu, R. C. J. Somerville, and S. Iacobellis, 1996: Single-column models and cloud ensemble models as links between observations and climate models. *J. Climate*, **9**, 1683-1697.

Somerville, R. C. J., S. F. Iacobellis, and W.-H. Lee, 1996: Effects of cloud-radiation schemes on climate model results. *World Resource Review*, **8**, 321-333.